

TEXTURE ANALYSIS OF 3D BLADDER CANCER CT IMAGES FOR IMPROVING RADIOTHERAPY PLANNING

William H. Nailon, Anthony T. Redpath and Duncan B. McLaren

University of Edinburgh Department of Oncology Physics
Directorate of Clinical Oncology, Western General Hospital
Crewe Road South, Edinburgh, EH4 2XU
Tel: +44(131) 537 3560, Fax: +44(131) 537 1092
E-mail: Bill.Nailon@luht.scot.nhs.uk

ABSTRACT

At present no single texture analysis approach can provide automatic classification to the accuracy required for radiotherapy applications. The method presented was developed to classify areas within the gross tumor volume (GTV), and other clinically relevant regions, on computerized tomography (CT) images. For eight bladder cancer patients, CT information was acquired at the radiotherapy planning stage and thereafter at regular intervals during treatment. Textural features (N=27) were calculated on regions extracted within the bladder, rectum and a region identified as clinically relevant. The sequential forward search (SFS) method was used to reduce the feature set (N=3). The results demonstrate the significant sensitivity of the reduced feature set for classification of any orthogonal CT image and the potential of the approach for radiotherapy applications.

Index Terms— Texture analysis, pattern recognition, computed tomography, radiotherapy

1. INTRODUCTION

The goal of radiotherapy is to deliver as high a dose of radiation as possible to diseased tissue whilst sparing healthy tissue. In radiotherapy planning, delineation of the GTV is based on visual assessment of CT images by a specialist radiation oncologist. With highly conformal radiotherapy now routine, faithful distinction of the GTV is paramount to limit normal tissue toxicity given the high radiation dose used to treat deep-seated tumors. However accurate definition of the GTV on CT images requires considerable clinical experience and as a consequence of this complex image interpretation process, significant inter- and intra-clinician variability has been observed in the contouring of tumors of the prostate, lung, brain and oesophagus [1]. A computer-assisted approach for classifying tissue and assisting in the delineation of the GTV

would therefore be of great benefit to clinicians. Several authors have investigated the use of two-dimensional (2D) texture analysis to establish an objective method for differentiating pathology on CT images [2, 3]. Extension to three-dimensions (3D) has also been performed on CT and other imaging modalities [4, 5, 6, 7, 8]. Here a 2D texture analysis methodology was developed that uses available 3D image information to determine textural features independently on axial, coronal and sagittal regions of interest on CT image data at the radiotherapy isocenter. In this way the methodology closely follows the manual approach used by clinicians to define the GTV.

2. TEXTURE ANALYSIS

In this work the classification of the bladder, rectum, and a clinically relevant region defined as other was investigated using computational methods based on statistical and fractal texture analysis. The statistical methods used were: first-order (FOS), based on analysis of the image histogram; second-order, based on gray-tone spatial dependence matrices (GTSDM); and higher-order, based on gray-tone run length matrices (GTRLM).

Fractals have been used to describe the degree of irregularity of a textured surface and to establish simple rules for the assembly of complex structures found in the natural world. The advantage of fractal-based approaches over statistical-based approaches is that only a single measure is required to describe the textural properties of an image, which offers a considerable computational benefit.

2.1. First-Order Statistics

From the distribution containing the occurrence probability of image gray-levels seven statistical features, commonly used to describe the properties of a distribution, were computed. These were: mean; variance; coarseness; skewness; kurtosis; energy; and entropy.

This work was supported by the Lothian University Hospitals NHS Trust.

2.2. Gray-Tone Spatial Dependence Matrices

Measures to detect second-order differences are based on the probability of finding a pixel that has gray-level i at a distance d_s and angle α from a pixel that has gray-level j . Calculating the probability measure over an image forms a GTSDM. Here, four GTSDMs were calculated in the directions, 0° ; 45° ; 90° ; 135° with $d_s = 1$. A set of 14 textural features was computed from the GTSDMs [8].

2.3. Gray-Tone Run Length Matrices

In this higher-order approach, GTRLMs contain information on the run of a particular gray-level combination (i, j) in a direction α . The number of pixels contained in a run is the run-length. Here, four GTRLMs were calculated in the directions 0° ; 45° ; 90° ; 135° on linearly adjacent pixels in the specified directions. A set of five textural features was computed from the GTRLMs [8].

2.4. Fractal Texture Analysis

A bespoke box-counting approach was used to estimate the fractal dimension of tumor regions. The box-counting dimension is closely related to the concept of self-similarity, which is implemented by dividing a self-similar structure into smaller elements, each a small replica of the original structure. This sub-division is used to characterize a structure by a self-similarity dimension. For the case when this approach is implemented using the box-counting method, the self-similarity dimension is the box-counting dimension. For any bounded subset A in \mathbf{R}^n the box-counting dimension D_b is defined as follows. Let $N_r(A)$ be the smallest number of sets of size r that cover A . Then,

$$D_b(A) = \lim_{r \rightarrow 0} \frac{\log N_r(A)}{\log(1/r)}. \quad (1)$$

Sub-dividing \mathbf{R}^n , which in this case was a CT image, into a lattice of grid size $r \times r$, it follows that $N_r(A)$ is the number grid boxes containing elements of interest in A . The box-counting dimension D_b and $N_r(A)$ are connected by the power law relation, $N_r(A) = 1/r^{D_b(A)}$.

3. CLINICAL DATA ACQUISITION

Computerized tomographic images for eight bladder cancer patients (six male and two female), treated with a radiation dose of 52.5 Gy (20 fractions/4 weeks) at the Edinburgh Cancer Center (ECC) were used in this study. The age range of the patients was 63 to 81 years and the mean 74 years. Prior to treatment each patient received a CT scan, with a presumed empty bladder, which was used to: define the tumor volume for treatment; define critical anatomical structures; determine the optimum radiation beam arrangement; and estimate the

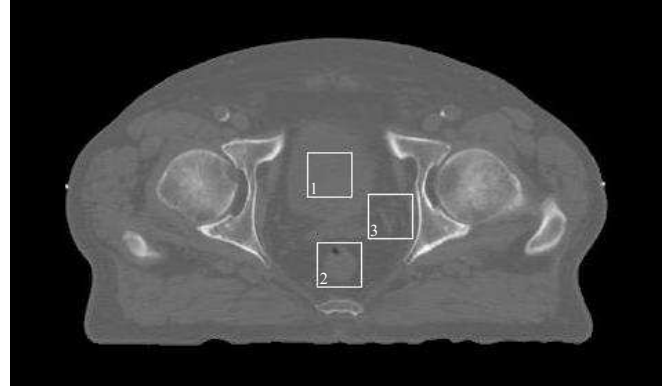


Fig. 1. Axial CT image through the pelvis showing showing: 1. Bladder, 2. Rectum, 3. Region of multiple pathology (Other). The image was acquired using a 3 mm slice thickness with a pixel size in the image plane of 0.977 mm.

dose delivered to the patient. During the course of treatment CT scanning was performed twice weekly. Seven patients were scanned using a 3 mm CT slice thickness and one patient using a 5 mm CT slice thickness. All repeat CT scans were registered against bony anatomy on the corresponding planning scan.

4. ALGORITHM

4.1. Feature Calculation Algorithm

Regions of interest (ROI), defined by selection of the smallest square region that adequately covered the rectum and would fit within the bladder, were calculated on the axial CT slice containing the radiotherapy isocenter. The control region, referred to as other, was chosen to contain multiple pathology. Fig. 1 shows a 3 mm axial CT image on which the ROIs are clearly visible. On each ROI, features (N=27) were calculated using FOS, GTSDM, GTRLM and the fractal approach described.

4.2. Feature Reduction

To reduce the complexity of the 27×3 feature matrix, features with limited classification power were removed using the SFS algorithm. For the original set of candidate features $Y = \{y_i | j = 1, 2, \dots, D\}$ the reduced feature set $X = \{x_i | i = 1, 2, \dots, d, x_i \in Y\}$ was selected by optimizing the criterion function $J(\cdot)$, which was chosen to be the minimum probability of error. For X the probability of correct classification (ξ) with respect to any combination was, $\Xi = \{\xi_i = |1, 2, \dots, d\}$. From this the minimum probability of error for the space spanned by (ξ) for each class ω_i was cal-

culated from,

$$E(\Xi) = \int [1 - \max(P(\omega_i|\xi))] p(\xi) d\xi. \quad (2)$$

4.3. Feature Clustering and Visualization

Sammon mapping was used to generate a 2D representation of the multi-dimensional feature space and assess the classification possible from different combinations of textural features. This is a non-linear technique used to transform a multi-dimensional pattern space into a lower dimensional pattern space in which multi-dimensional inter-pattern distances are preserved. For a set $\{\mathbf{x}_i\}$ of n d -dimensional patterns, where $d_{i,j}$ represents the distance between patterns \mathbf{x}_i and \mathbf{x}_j in d -dimensional pattern space, there exists a mapping to a lower dimensional pattern space m , where ($m < d$), and $D_{i,j}$ is the distance between \mathbf{x}_i and \mathbf{x}_j in m -dimensional pattern space. The mean-square-error between the two distance measures is defined as,

$$E = \frac{1}{\sum \sum d(i,j)} \sum \sum \frac{[d(i,j) - D(i,j)]^2}{d(i,j)}, \quad (3)$$

where $\sum \sum$ are over the set $\{(i,j) : 1 \leq i < j \leq n\}$.

5. RESULTS AND DISCUSSION

The performance of the technique was investigated under two test conditions. In the first all of the available features (N=27) were used to classify bladder, rectum and other pathology on axial, coronal and sagittal CT image slices at the treatment isocenter. In the second a reduced feature set (N=3) was used to classify the same data. The classification results achieved using all of the available features are shown in Fig. 2, 3, and 4. The classification results achieved using the three most significant features are shown in Fig. 5, 6, and 7.

The texture analysis approach presented has been specifically designed to deal with classification of calibrated CT image data, which guarantees the relationship between CT Hounsfield units and electron densities used in radiotherapy planning. No significant discrimination was observed for the classification of the bladder, rectum and other region using all of the available features. This is shown in Fig. 2, 3, and 4. Significant discrimination between the three groups was achieved using the reduced feature set as shown in Fig. 5, 6, and 7. The best three features, all from the GTSDM approach, were: f_1 , angular second moment (ASM); f_3 , correlation; and f_4 variance. Importantly for this work, coincident classification of the textural feature data in each orthogonal plane has the necessary sensitivity and specificity for radiotherapy applications and has the potential to form the basis of a computer-based procedure for accurate delineation of the GTV on CT, magnetic resonance (MR) and positron emission tomography (PET) images. This is vitally important for

two reasons. Firstly to determine the optimum size and shape of the GTV, which has been shown to be different when defined by different oncologists [1]. Secondly, as stated by the International Commission on Radiation Units and Measurements (ICRU), the GTV may seemingly be different in size and shape, sometimes significantly, depending on what examination technique is used for evaluation.

6. CONCLUSION

Estimating orthogonal textural properties at the radiotherapy isocenter offers information on pathology that is presently not available. The lesson learned is that texture analysis can be used to differentiate pathology on CT in any of the orthogonal image planes. Further research is required to establish the influence of the many parameters that can be adjusted in the second- and higher-order approaches.

7. REFERENCES

- [1] C. Weltens and J. Menten et al., "Interobserver variations in gross tumor volume delineation of brain tumors on CT and impact of MRI," *Radiother Oncol*, vol. 60, no. 1, pp. 49–59, 2001.
- [2] M.N. Prasad and Sowmya et al., "Multilevel emphysema diagnosis of HRCT lung images in an incremental framework," *In Proc. SPIE Medical Imaging*, vol. 5370, pp. 42–50, May 2004.
- [3] R. Uppaluri and T. Mitsa et al., "Quantification of pulmonary emphysema from lung computed tomography images," *Am. J. Respir. Care Med*, vol. 156, no. 1, pp. 248–254, July 1997.
- [4] D. Xu and A.S. Kurani et al., "Run-length encoding for volumetric texture," in *4th IASTED Int. Conf. on Visualization, Imaging and Image Processing*, 2004.
- [5] K. Jafari-Khouzani and H. Soltanian-Zadeh et al., "Comparison of 2D and 3D wavelet features for TLE lateralization," *In Proc. SPIE Medical Imaging*, vol. 5369, no. 1, pp. 593–601, April 2004.
- [6] A.S. Kurani and D. Xu et al., "Co-occurrence matrices for volumetric data," in *7th IASTED Int. Conf. on Computer Graphics and Imaging*, 2004.
- [7] V.A. Kovalev and F. Kruggel et al., "Three-dimensional texture analysis of MRI brain datasets," *IEEE Trans. Med. Imag.*, vol. 20, no. 5, pp. 424–433, 2004.
- [8] Y. Xu and M. Sonka et al., "MDCT-based 3-D texture classification of emphysema and early smoking related lung pathologies," *IEEE Trans. Med. Imag.*, vol. 25, no. 4, pp. 464–475, 2006.

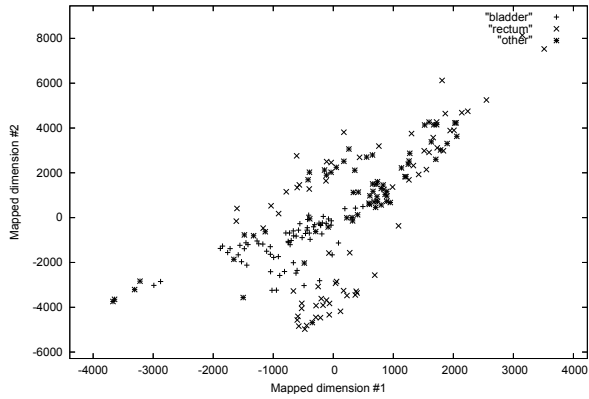


Fig. 2. Classification of axial data using all features.

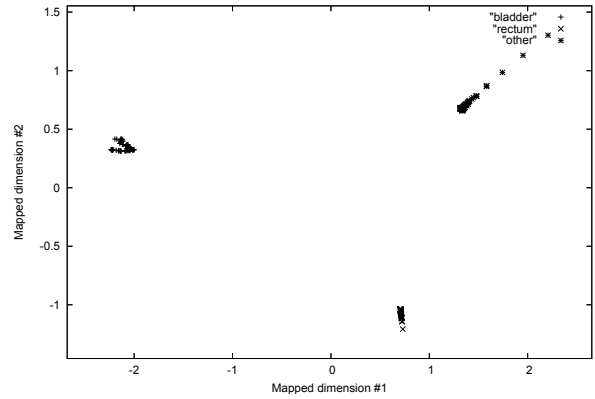


Fig. 5. Classification of axial data using three features.

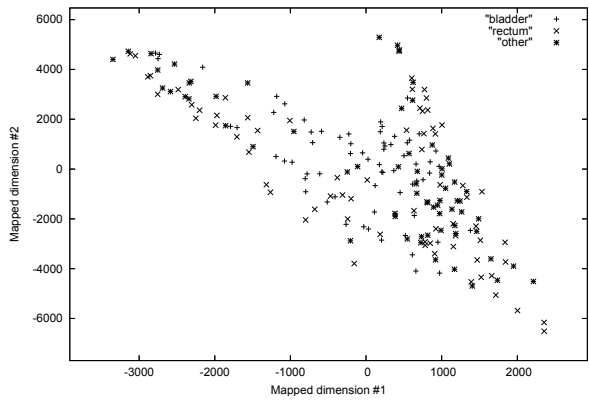


Fig. 3. Classification of coronal data using all features.

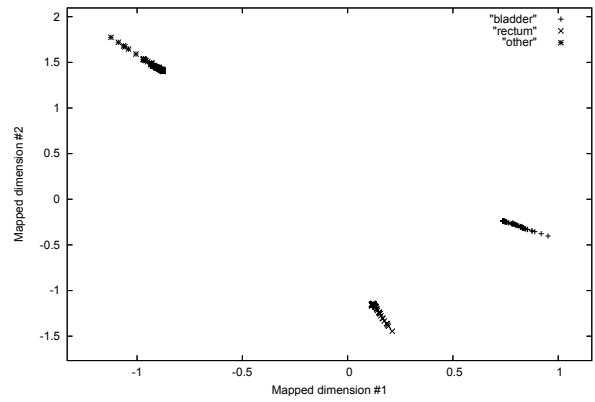


Fig. 6. Classification of coronal data using three features.

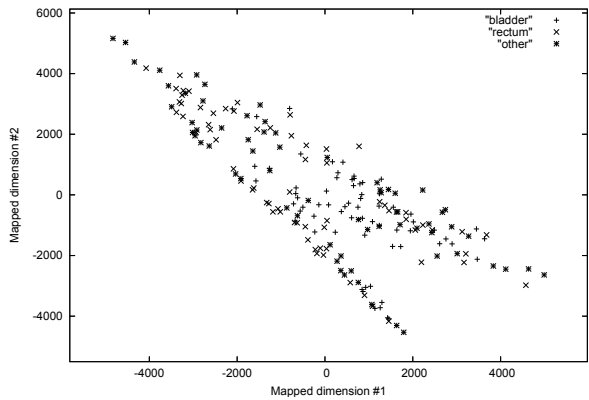


Fig. 4. Classification of sagittal data using all features.

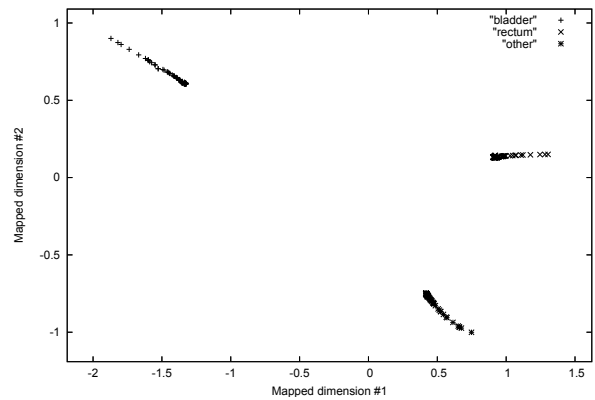


Fig. 7. Classification of sagittal data using three features.